2017 IEEE International Conference on
Autonomous Robot Systems and Competitions (ICARSC)
April 26-28, Coimbra, Portugal

Efficient Localization based on Scan Matching with a Continuous Likelihood Field

Eurico Pedrosa, Artur Pereira, Nuno Lau

***Abstract*—This paper presents a fast scan matching approach to mobile robot localization supported by a continuous likelihood field. The likelihood field plays a central role in the approach, as it avoids the necessity to establish direct correspondences; it is the connection link between scan matching and robotic localization, and it provides a reduced computational complexity. Scan matching is formulated as a non-linear least squares problem and solved by the Gauss-Newton and Levenberg-Marquardt methods. Furthermore, to reduce the influences of outliers during optimization, a loss function is introduced. The proposed solution was evaluated using a publicly available dataset and compared with AMCL, a state-of-the-art localization algorithm. Our proposal shows to be a fast and accurate localization algorithm suitable for any type of operation.**

I. Introduction

Mobile robot localization, or *pose estimation*, is the problem of ascertaining the pose of a robot relative to a given representation (i.e. map) of the environment. More than two decades ago, Cox [1] considered it to be the fundamental problem to provide a mobile robot with autonomous capabilities and it holds true up to our days. Many robotic tasks requires knowledge about the location of the robot and of the objects that are being manipulated. Sadly, the pose of the robot can *not* be sensed directly. The problem with mobile robot localization is that most robots do not have pose measuring sensors free of noise, therefore, the pose has to be inferred from other data. However, a single sensor measurement is typically not enough to determine the pose of the robot, therefore, the data has to be integrated over time considering all sources of information (sensors and actions) for pose determination.

The scan matching approach, when used for localization, tries to find the relative translation t and rotation θ between a reference pose and the current pose of the robot. This is achieved by overlapping the current map (or its subset) relative to the reference pose and one range scan taken at the actual pose of the robot. Scan matching has the advantage of estimating robot poses with high precision and, because it is bounded to small perturbations of sensor scans, it can be computed with efficiency [2].

The application of scan matching to mobile robot localization relies on matching a set of points $\{\mathbf{p}_i\}$ against a reference surface $\mathcal{S}^{\text{ref}}$, in order to find the planar roto-translation $\mathbf{q} = (\theta, t)$ that minimizes a function of the distances of the roto-translated points $\{\mathbf{q} \oplus \mathbf{p}_i\}$ to their projection on $\mathcal{S}^{\text{ref}}$. Here, $\oplus$ is the roto-translation operator, such that

$$(\theta, t) \oplus \mathbf{p}_i \triangleq R(\theta)\mathbf{p}_i + t \;, \tag{1}$$

where $R(\theta)$ is the rotation matrix. Using an Euclidean projector on $\mathcal{S}^{\text{ref}}$, denoted $\Pi(\mathcal{S}^{\text{ref}}, \cdot)$, the minimization problem can be defined by

$$\min_{\mathbf{q}} \sum_i \left\| \mathbf{q} \oplus \mathbf{p}_i - \Pi(\mathcal{S}^{\text{ref}}, \mathbf{q} \oplus \mathbf{p}_i) \right\|^2 \;. \tag{2}$$

To solve this minimization problem, several Iterative Corresponding Point (ICP) variants have been proposed [3], [4], [5], [6]. But, as noted by Burguera et al. [7], they may suffer from two important drawbacks: incorrect correspondences from the projector $\Pi(\mathcal{S}^{\text{ref}}, \cdot)$ and poor convergence as a side effect of inconsistent correspondences.

In this paper, we propose the use of a *fast* scan matching approach, from our previous work [8], for localization (section II) with a *likelihood field* as measurement model (section III). The *likelihood field* has a central role in this work: it addresses the drawbacks of the ICP algorithm, by avoiding the direct establishment of correspondences [7]; and it is the element that connects scan matching to mobile robot localization. Also, to reduce the discretization effect of the *likelihood field*, we will introduce a *likelihood field* with a continuous codomain. Once the scan matching formulation is in place we will solve it using *non-linear least squares* optimization methods (section IV).

Our approach to localization was validated through a set of experiments. Their description and the obtained results are presented in section V. Finally, this paper presents some related work (section VI) and our conclusions (section VII).

II. Maximum Likelihood Pose Estimation

Let x_t be the robot state at time t and z_t the measurements. The control u_t at time t determines the change of state from $t-1$ to t. The distribution that models the robot pose estimate can be simplified by

$$p(x_t \mid z_{1:t}, u_{1:t}) \propto p(z_t \mid x_t, m)\, p(x_t \mid x_{t-1}, u_t) \tag{3}$$

The first term, $p(z_t|x_t, m)$, represents the *measurement model* that expresses how likely is a particular measurement if the robot's pose and the map are known. The term $p(x_t|x_{t-1}, u_t)$ represents the *motion model* that describes the probability of the pose x_t after executing the control u_t.

All authors are with Intelligent Robotics and Intelligent Systems Lab (IRIS), Institute of Electronics and Informatics Engineering of Aveiro (IEETA), Department of Electronics, Telecommunications and Informatics (DETI) - University of Aveiro, Portugal email: {efp,artur,nunolau}@ua.pt

978-1-5090-6234-8/17/$31.00 ©2017 IEEE

Our proposal to solve the localization problem is based on the calculation of the maximum likelihood of $p(z_t|x_t, m)$. The motion model is used as an initial hint for x_t, and treated as a constant. This assumption is valid because we are considering a local search approach, and the accurate measurements from a LIDAR sensor causes the product of (3) to be dominated by the observation likelihood [9]. Thus, the pose estimation can be reduced to

$$\hat{x}_t = \max_{x_t} p(z_t \mid x_t, m) \ . \tag{4}$$

The measurement z_t is defined by a set of points $\{\mathbf{p}_t^i\}$, thus, the resulting calculation is the collection of probabilities $p(\mathbf{p}_t^i|x_t, m)$, where $\mathbf{p}_t^i$ is the ith measurement. Assuming conditional independence between measurements, the measurement model probability is given by:

$$p(z_t \mid x_t, m) = \prod_i p(\mathbf{p}_t^i \mid x_t, m) \ . \tag{5}$$

Introducing (5) into (4) the maximum likelihood estimate can be rewritten as

$$\hat{x}_t = \max_{x_t} \prod_i p(\mathbf{p}_t^i \mid x_t, m) \ . \tag{6}$$

As it can be numerically unstable to solve (6), a usual approach is to use the log-likelihood. The problem can now be formulated as a minimization of the negative log-likelihood of our measurement model:

$$\hat{x}_t = \min_{x_t} \sum_i - \ln \left[p(\mathbf{p}_t^i \mid x_t, m) \right] \ . \tag{7}$$

The next step is to select a proper measurement model for the pose estimation, and our choice is the *likelihood field*.

The *likelihood field* was designed as a measurement model with smoother results and computationally more efficient than the *beam model* [10]. Efficiency is achieved by caching the likelihood values of the reference surface $\mathcal{S}^{\text{ref}}$ in a discrete volumetric grid. Access to the values is provided by a function

$$l : \mathbb{R}^n \to \mathbb{R} \tag{8}$$

such that $l(\hat{x}_t \oplus \mathbf{p}_i)$ returns the likelihood of the point $\mathbf{p}_i$ roto-translated by $\hat{x}_t$, the current pose of the robot.

III. Likelihood Field as Measurement Model

Because we are dealing with measurements taken from a LIDAR sensor, the calculation of the *probability density function* (PDF) of each sample z_t should, in principle, consider which surface of the map is visible from the pose x_t. The *beam model* [10] does this by applying an expensive ray-casting operation. To avoid this expensive operation we adopted the *likelihood field* (LF) model that, although neglecting visibility and occlusion effects, if constructed properly, can give smoother results at a lower computational cost. The LF is defined as a function of x–y-coordinates expressing the likelihood of object detection [10]. Although not a proper PDF, we will demonstrate its use in pose estimation with scan matching, more specifically, how it can be used as the measurement model in localization.

Lets us define the LF function $l(\mathbf{p})$ as:

$$l(\mathbf{p}) = \exp(-\|\mathbf{p} - \Pi(m, \mathbf{p})\|^2) \tag{9}$$

where $\mathbf{p} = [\mathbf{p}_x, \mathbf{p}_y]^T$ and $\Pi(m, \cdot)$ is the Euclidean projector on m to the closest occupied cell. To be a proper LF, $l(\mathbf{p})$ must have the following property: the closer a point $\mathbf{q}$ is to its projection $\Pi(m, \mathbf{p})$ the more likely it is to be measured. This property is fulfilled by the fact that the value of $l(\mathbf{p})$ is the exponent of the negative squared Euclidean distance between $\mathbf{p}$ and the closest object in m, which increases in value as the Euclidean distance decreases.

We can realize that (9) corresponds to the non normalized PDF of a Gaussian distribution with identity covariance matrix. Turning the LF function into a PDF is a matter of introducing a normalization factor η:

$$\begin{aligned} f(\mathbf{p}) &= \eta l(\mathbf{p}) \\ &= \eta \exp(-\varepsilon^2(\mathbf{p})) \end{aligned} \tag{10}$$

with

$$\varepsilon(\mathbf{p}) = \|\mathbf{p} - \Pi(m, \mathbf{p})\| \tag{11}$$

as the Euclidean distance to the nearest neighbor. This new obtained PDF (10) can now be used as our measurement model. Assuming that all LIDAR scans are independent, the measurememt model for our maximum likelihood pose estimation is given by

$$p(z_t \mid x_t, m) = \prod_i \eta \exp(-\varepsilon^2(x_t \oplus \mathbf{p}_t^i)) \ . \tag{12}$$

A. Continuous Likelihood Field

The low computational cost of the likelihood field results from the discretization of the environment in the form of a grid where each cell contains pre-computed likelihood of a measurement. Kohlbrecher et al. [11] noted that discrete representations limit the precision that can be achieved, as an improvement, they propose the use of an interpolation scheme that allows sub-cell accuracy through bilinear filtering. The same interpolation scheme is applied to the Euclidean distance grid $\hat{\varepsilon}$, the discrete version of the Euclidean distance ε that is part of the likelihood field. Given a continuous coordinate $\mathbf{p}_\varepsilon = [x, y]$ in grid coordinates with $x, y \in [0, 1)$, the value of the Euclidean distance is computed from the four closest integer coordinates $\mathbf{p}_{00..11}$. It should be noted that the cells of the grid are organized in a regular grid with spacing equal to 1 in grid coordinates. The effective formula for value interpolation yields

$$\hat{\varepsilon}(x, y) \approx \begin{bmatrix} 1-x & x \end{bmatrix} \begin{bmatrix} \varepsilon(\mathbf{p}_{00}) & \varepsilon(\mathbf{p}_{01}) \\ \varepsilon(\mathbf{p}_{10}) & \varepsilon(\mathbf{p}_{11}) \end{bmatrix} \begin{bmatrix} 1-y \\ y \end{bmatrix} \ . \tag{13}$$

Inherent to this scheme is that values from the grid cells are now samples from a continuous function. Instead of pre-computing the likelihood for each cell, only the Euclidean distance grid is pre-computed and then used to calculate the likelihood as a continuous value, e.g Figure 1.

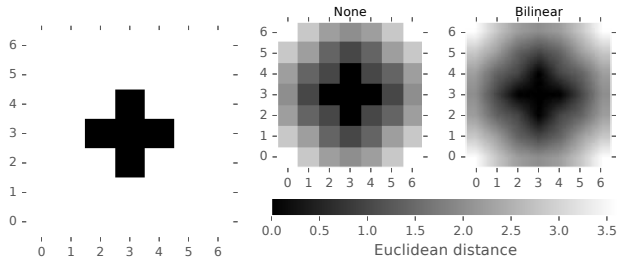

(a) (b)

Fig. 1. Interpolation scheme for a continuous likelihood field. a) Example of an environment occupancy map that models free space (white) and obstacles (black). b) Corresponding distance map, here two schemes are used, one without interpolation that represents the typical discrete Euclidean distance map, the second scheme employs a bilinear interpolation on top of the discrete distance map.

IV. Non-Linear Least Squares Optimization

The use of *non-linear least squares* to solve the minimization problem introduced by the formal definition of scan matching in (2) is a common approach, as, by definition, *least squares* tries to minimize the sum of the squared errors of our objective function w.r.t its parameters.

To obtain the estimation of x_t we need to solve the minimization (7). However, it lacks the least squares formulation found in the scan matching definition of (2), and subsequently it can not be solved using least squares optimization. Therefore, minimization of (7) needs to be converted to an equivalent least squares formulation. This can be achieved by replacing the measurement model in (7) with the measurement model based on the LF:

$$\begin{aligned}\hat{x}_t &= \min_{x_t} \sum_i -\ln\left[\eta \exp(-\varepsilon^2(x_t \oplus \mathbf{p}_t^i))\right] \\ &= \min_{x_t} -n\ln\eta + \sum_i \varepsilon^2(x_t \oplus \mathbf{p}_t^i) \\ &= \min_{x_t} \sum_i \varepsilon^2(x_t \oplus \mathbf{p}_t^i)\ . \end{aligned} \tag{14}$$

The term $-n\ln\eta$ can be safely ignored because it is constant and thus does not influence the minimization.

Up until now, in this paper, localization and scan matching had been presented as two different concepts. The introduction of the LF into the localization problem has the consequence of converting the localization problem into a scan matching problem and, as a result, it can now be solved using least squares. Our approach tries to find the pose $\hat{x}_t = [x, y, \theta]^T$ that best aligns the endpoints $\mathbf{p}_t$ of the scan with the local surface of the map m. Due to the use of the LF there is no need to find correspondences for the endpoints. Also, because scans are aligned with the map m, there is an implicit matching with all previous scans.

A common approach to solve a *non-linear least squares* optimization is to use the Gauss-Newton method [12]. The method consists in iteratively updating the pose estimate with the rule

$$\hat{x}_t^{i+1} = \hat{x}_t^i + \Delta\mathbf{x}\ , \tag{15}$$

where at each iteration the update step $\Delta\mathbf{x}$ is obtained by solving the *normal equation*:

$$(\mathbf{J}^T\mathbf{J})\Delta\mathbf{x} = -\mathbf{J}^T\varepsilon(\hat{x}_t \oplus \mathbf{p}_t) \tag{16}$$

with

$$\mathbf{J} = \mathbf{J}_\varepsilon\mathbf{J}_\oplus = \frac{\partial\varepsilon(\hat{x}_t \oplus \mathbf{p}_t)}{\partial\hat{x}_t \oplus \mathbf{p}_t}\frac{\partial\hat{x}_t \oplus \mathbf{p}_t}{\partial\hat{x}_t}$$

The method stops when convergence is found or when a maximum number of iterations is reached. The initial hint of $\hat{x}_t^{i=1}$ if provided by the previous estimate $\hat{x}_{t-1}$ plus the displacement of the odometry between $t-1$ and t. To prevent unnecessary estimates, for example when there is no motion, the estimate of the pose is only carried when a certain amount of motion exists. The motion is divided into its translation ρ and rotational ϑ components. The pose estimation is only triggered when a threshold is reached in any of the components.

A variant of Gauss-Newton, called Levenberg-Marquardt (LM), is also used as an alternative method to obtain the estimates. It changes the normal equation as follows:

$$(\mathbf{J}^T\mathbf{J} + \mu\mathbf{I})\Delta\mathbf{x} = -\mathbf{J}^T\varepsilon(\hat{x}_t \oplus \mathbf{p}_t)\ , \tag{17}$$

where μ is a *damping* parameter that affects the optimization. For all $\mu > 0$, it is guaranteed that $\Delta\mathbf{x}$ is in the direction of the steepest descent. If $\mu \to 0$, the method falls back into the pure Gauss-Newton, whereas if $\mu \to \infty$ the gradient descent is used. Furthermore, the update $x_t + \Delta\mathbf{x}$ is only performed if there is a significant residual error reduction. Upon success, μ is decreased, otherwise μ is increased. The reasoning behind this heuristic is that the quadratic convergence of Gauss-Newton is good near the minimum, but not so good far from it, where gradient descent has a better behaviour.

A. Handling Outliers

The incorrect modelling of the measurement likelihood will likely create disturbances in the maximum likelihood estimate [13], such as the maximum likelihood pose estimate. The common cause for this type of mismodelling is the failure to take into account the existence of *outliers* (abnormal data values cause e.g. by unexpected features). Such example is the use of the Gaussian distribution to model the measurement likelihood (Figure 2).

In mobile robot localization, outliers are naturally present in range scans. To address this problem we can use a robustified version of the least squares problem presented in (14):

$$\hat{x}_t = \min_{x_t} \sum_i \rho_i\left(\varepsilon^2(x_t \oplus \mathbf{p}_t^i)\right)\ , \tag{18}$$

where ρ is a *loss function* used to reduce the influence of outliers. The advantage of this formulation is that we can maintain the original measurement model, i.e. the likelihood

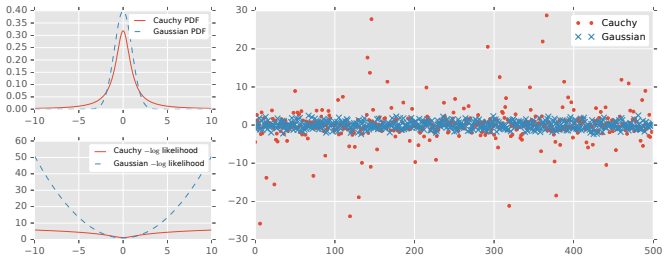

Fig. 2. Not all bell-shaped measurement distributions are Gaussians [13]. The Cauchy distribution, although with a narrower peak and broader tail, is not very different from the Gaussian distribution (*top left*) but their negative log likelihood are very different (*bottom left*), in fact the Cauchy distribution accounts for larger deviations (outliers) than the Gaussian one (*right*).

field. Following [13] proposal, we use the *Cauchy* loss function as ρ:

$$\rho(x^2) = \frac{c^2}{2} \ln\left(1 + \frac{x^2}{c^2}\right) \tag{19}$$

$$\rho'(x) = \frac{1}{x}\frac{d\rho_i}{dx} = \frac{1}{1 + \frac{x^2}{c^2}} \,. \tag{20}$$

where c is the factor that controls the behavior of the loss function. The minimization process follows the same steps as previously discussed but with the following substitutions:

$$\overline{\mathbf{J}}_i = \sqrt{\rho_i'}\,\breve{\mathbf{J}}_i \quad \wedge \quad \overline{\varepsilon}_i = \sqrt{\rho_i'}\,\varepsilon(\hat{x}_t \oplus \mathbf{p}_t^i)$$
$$(\overline{\mathbf{J}}^T\overline{\mathbf{J}})\Delta\mathbf{x} = -\overline{\mathbf{J}}^T\overline{\varepsilon} \tag{21}$$

This addition improves the estimation of the robot pose x_t and makes the approach more tolerant to outliers [13].

V. Experimental Results and Evaluation

We seek to evaluate the quality of the pose estimates generated by our localization solution as well its computational efficiency. For that purpose, we used a set of publicly available datasets, and ran them through our algorithm. The datasets in question are the ACES Building, the Intel Research Lab, the MIT CSAIL Building, the Freiburg Building 079 and the MIT Killian Court. All experiments were run in a computer with an Intel Core i7 2.8GHz and 16GiB of RAM, and all data was used without pre-processing.

To better evaluate our result we need to define a comparison baseline. For that purpose we chose the Adaptive Monte Carlo Localization (AMCL) [14], a localization algorithm based on a particle filter with an adaptive number of samples. This decision is based on the fact that AMCL is a popular state-of-the-art localization algorithm widely used in mobile robotics. To distinguish our solution from AMCL, we will refer to it as Scan Matching or SM. Additionally, for SM, results for two optimization strategies, i.e. Gauss-Newton and Levenberg-Marquardt, will be presented and evaluated.

For both solutions, an update only occurs after accumulating $\rho = 0.2m$ translation motion or after accumulating $\vartheta = 0.5rad$ rotational motion. In AMCL's particle filter a minimum of 500 and a maximum of 5000 particles are used. Both solutions use a likelihood field measurement model, but with the difference that AMCL uses 30 scan rays for evaluation while our proposal uses the complete set of scan rays (180 per scan).

A. Trajectory Validation

The sum of all pose estimates results in the trajectory traveled by the mobile robot. Sny localization algorithm should obtained a trajectory as close as possible to the real trajectory. The best method to evaluate the obtained trajectories is to compare them with ground-truth data. Unfortunately, a ground-truth for the selected datasets is not available, but it is still possible to assess the validity of a trajectory. A trajectory is considered to be fully (or partially) valid when: for the same dataset the trajectories resulting two different algorithms are similar; and the trajectory only crosses free space.

For all datasets the obtained trajectories for SM and AMC are valid and similar, although there is a localized and a broader exception. The localized exception is found in the CSAIL dataset. Here, on a contained area of the map, the AMCL algorithm fails to maintain the trajectory inside free space while our solution maintains the correct trajectory, as depicted in Figure 3(a).

The broader exception if found in the Fr079 dataset. There are considerable differences between our proposal's trajectory and AMCL's at certain areas of the map, e.g. Figure 3(b). Nonetheless, the trajectory of our solution is always contained in free space while AMCL's is not. The odometry provided by the dataset contains considerable errors that frequently leads to erroneous pose estimations in most localization algorithms. By increasing the pose estimation frequency our solution was able to handle the error in the odometry. The same increase was used in the AMCL algorithm, but it still failed to handle the errors in the odometry.

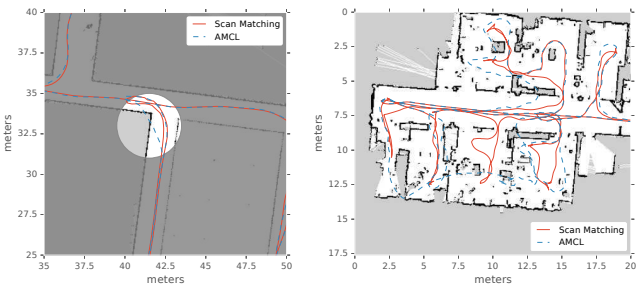

(a) CSAIL (b) Fr079

Fig. 3. Erroneous deviation of AMCL's trajectories. (a) Localized trajectory deviation in the CSAIL dataset. (b) Considerable amount of trajectory deviations in the Fr079 dataset due to errors in the odometry.

B. Accuracy of Pose Estimates

As already stated, the best method to evaluate the accuracy of the pose estimates would be to compare them with a ground-truth data, unfortunately one is not available. Instead of directly evaluating the pose estimate we propose to evaluate how well the current scan matches the map at the estimated

pose. We reason that the scan matching error correlates with the accuracy of the pose estimate, the lower the scan matching error the higher the accuracy of the estimate. An example is presented in Figure 4.

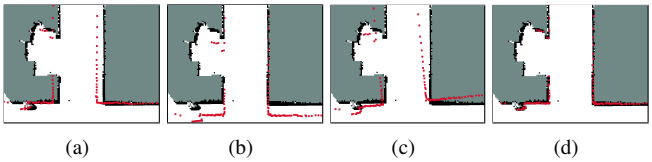

(a) (b) (c) (d)

Fig. 4. Pose estimate accuracy inferred from scan-to-map matching errors. (a) Pose estimate with errors in the Y axis. (b) Pose estimate with errors in the X axis. (c) Pose estimate with angular errors. (d) Pose estimate with the smallest scan matching errors.

The metric used to (indirectly) assess the accuracy of each pose estimate is the root mean square error (RMSE) of the scan matching defined as

$$\text{RMSE} = \sqrt{\frac{1}{n}\sum_{i=1}^{n}\varepsilon^2(x_t \oplus \mathbf{p}_t^i)} \ . \tag{22}$$

where the error is given by the Euclidean distance between a measurement end-point and the closest object in the map. An overview of the obtained errors for each algorithm, grouped by dataset, is presented in Figure 5. Our scan matching solution has a lower error than AMCL for most datasets, and, when comparing with Gauss-Newton strategy, our proposal has constantly lower error than AMCL.

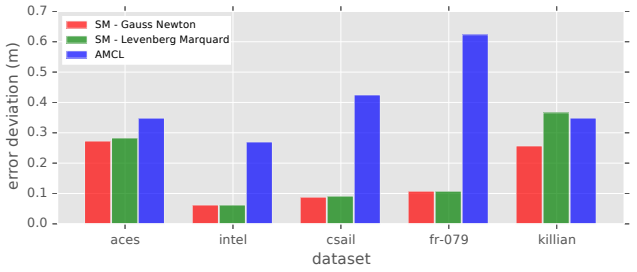

Fig. 5. Root mean square error overview. For each algorithm, grouped by dataset, the 95% percentile value is shown (a lower value is better).

C. Computational Efficiency Analysis

We are also interested in analyzing the computational efficiency of our localization solution. More specifically, the mean processing time (or update time) between each scan s_{proc} and the mean number of iterations needed during optimization.

The execution times of our solution and AMCL's are summarized in Table I. The scan matching solution offers some interesting results in terms of computational efficiency. Not only it is, on average, faster than AMCL but the gamut of execution times is considerable shorter. The Levenberg-Marquardt optimization strategy has an execution time that is regularly slightly above Gauss-Newton strategy. When using the Levenberg-Marquardt optimization strategy with the Killian dataset, the optimizer, in an isolated event, has poor convergence, which results in abnormal maximum execution time when compared with other datasets.

TABLE I
MEAN EXECUTION TIMES AND RESPECTIVE STANDARD DEVIATION, AND MIN-MAX VALUES FOR ALL DATASETS, GROUPED BY ALGORITHM.

	Scan Matching - GN		Scan Matching - LM	
	$s_{\text{proc}}\ ms$	min-max	$s_{\text{proc}}\ ms$	min-max
aces	0.67 ± 0.28	$0.19 - 2.00$	0.96 ± 0.34	$0.33 - 3.02$
intel	0.56 ± 0.18	$0.24 - 1.95$	0.78 ± 0.24	$0.33 - 2.64$
csail	1.40 ± 0.61	$0.35 - 5.90$	1.88 ± 0.75	$0.65 - 7.50$
fr079	0.99 ± 0.37	$0.28 - 4.53$	1.40 ± 0.48	$0.45 - 5.81$
killian	0.66 ± 0.32	$0.18 - 5.75$	1.16 ± 0.80	$0.17 - 41.5$

AMCL

	$s_{\text{proc}}\ ms$	min-max
aces	3.98 ± 4.78	$2.62 - 57.42$
intel	13.5 ± 11.9	$7.68 - 144.0$
csail	5.14 ± 7.76	$2.55 - 65.47$
fr079	5.56 ± 7.85	$2.60 - 85.75$
killian	2.91 ± 0.51	$2.56 - 34.11$

All datasets have a data rate of approximately 6Hz (a $166ms$ period) and that means that our scan matching solution and AMCL are always capable of estimating the pose in real-time. However, nowadays, LIDAR sensors have data rates of 25Hz (a $40ms$ period) or even 50Hz (a $20ms$ period) which may hinder AMCL's capability to process data in real-time, while our solution still maintains the real-time property.

In AMCL, the number of particles has a direct influence in its computational efficiency, the higher the number of particles the higher the processing time. Because this number adapts to the variance in the particle set, areas in the map with higher uncertainty (or error) trigger an increase in the number of particles that results in higher processing times. This tells us that, for most datasets, AMCL needs to continuously trade computational efficiency for better pose estimates.

In our scan matching solution, the number of optimizations has a clear impact in its computational efficiency - the lower the number of iterations, the higher the computational efficiency. A summary of the number of iterations of our solution, per strategy, is shown in Table II. On average, our solution has a reduced number of iterations during optimization, specially when using the Gauss-Newton strategy, and as result it has a high computational efficiency. The reduced number of iterations is also an indication that the emplaced non-linear least squares optimization has good convergence. As previously mentioned, the Levenberg-Marquardt strategy has a one-time event in the Killian dataset where its convergence is poor.

VI. Related Work

Early localization algorithms based on scan matching can be tracked back to Lu and Milios [15]. In their work they describe several approaches for scan-matching using ICP-like methods. The objective of the ICP and its variants is the same, to iteratively find the transformation between the current scan and a reference that best fits the point correspondence criterion. The differences are how the transformation is found and what point correspondence criterion is used.

TABLE II
MEAN NUMBER OF OPTIMIZATION ITERATIONS AND RESPECTIVE STANDARD DEVIATION, AND MIN-MAX VALUES FOR ALL DATASETS, GROUPED BY ALGORITHM.

	Scan Matching - GN		Scan Matching - LM	
	# iterations	min-max	# iterations	min-max
aces	6.93 ± 3.34	$1 - 24$	12.30 ± 4.60	$3 - 37$
intel	5.70 ± 2.14	$1 - 22$	9.88 ± 3.63	$3 - 32$
csail	8.10 ± 4.03	$1 - 40$	13.37 ± 5.86	$3 - 58$
fr079	5.47 ± 2.24	$1 - 25$	9.65 ± 3.52	$2 - 34$
killian	5.99 ± 3.40	$1 - 44$	13.84 ± 9.26	$1 - 488$

In the literature, we can find a significant number of ICP variants for scan matching. For example, Censi [16] proposes a point-to-line correspondence with closed-form minimization while Diosi and Kleeman [17] do point correspondence in the polar's coordinate system. Other methods try to avoid explicit point correspondence, The Normal Distribution Transformation (NDT) [18] subdivides the 2D plane into cells and assigns a normal distribution that models the probability of measuring a point. Similarly, Burguera et al. [7] uses a likelihood field as measurement model, Lauer et al. [19] and Dantanarayana et al. [20] rely on distance functions for scan matching.

Scan matching algorithms are typically *local* algorithms. However, there are solutions that operate globally, such as the Hough scan matching [21] that operates in the Hough domain and correlative scan matching [22][23] that globally searches for the best cross-correlation between the a scan and the map.

VII. CONCLUSION

This paper presents a localization algorithm for mobile robots based on scan matching supported by a likelihood field. The localization problem is first introduced as a maximum likelihood pose estimation, and by introducing a continuous likelihood field as the measurement model the it is converted into an isometric scan matching problem solved by non-linear least squares. In the carried experiments, our scan matching proposal has a high computational efficiency that results from good convergence of the optimization process. Furthermore, when compared with AMCL, a state-of-the-art localization algorithm, our solution not only provides pose estimates with better accuracy for all experiments but also has full valid trajectories, not partially valid like in some experiments with AMCL. The end result is an accurate localization algorithm for mobile robots with a high computational efficiency that makes it suitable for tasks with real-time requirements.

ACKNOWLEDGMENT

This research is supported by: Portuguese National Funds through Foundation for Science and Technology (FCT), in the context of the project UID/CEC/00127/2013; and by European Union's FP7 under EuRoC grant agreement CP-IP 608849.

REFERENCES

[1] I. J. Cox, "Blanche-An Experiment in Guidance and Navigation of an Autonomous Robot Vehicle," *Robotics and Automation, IEEE Transactions on*, vol. 7, no. 2, pp. 193–204, 1991.

[2] J. S. Gutmann, W. Burgard, D. Fox, and K. Konolige, "An Experimental Comparison of Localization Methods," in *Proceedings. 1998 IEEE/RSJ International Conference on Intelligent Robots and Systems. Innovations in Theory, Practice and Applications*. IEEE, 1998, pp. 736–743.

[3] F. Lu and E. Milios, "Globally Consistent Range Scan Alignment for Environment Mapping," *Autonomous Robots*, vol. 4, pp. 333–349, 1997.

[4] S. T. Pfister, K. L. Kriechbaum, S. I. Roumeliotis, and J. W. Burdick, "Weighted Range Sensor Matching Algorithms for Mobile Robot Displacement Estimation." in *Proc. of the IEEE Int. Conf. on Robotics & Automation (ICRA)*, vol. 2, Washington, DC, USA, May 2002, pp. 1667–1674.

[5] L. Montesano, J. Minguez, and L. Montano, "Probabilistic Scan Matching for Motion Estimation In Unstructured Environments," in *Proc. of the IEEE/RSJ Int. Conf. on Intelligent Robots and Systems (IROS)*, August 2005, pp. 3499–3504.

[6] A. Censi, "An ICP variant using a point-to-line metric," in *Proc. of the IEEE Int. Conf. on Robotics & Automation (ICRA)*, Pasadena, CA, USA, May 2008, pp. 19–25.

[7] A. Burguera, Y. González, and G. Oliver, "On the Use of Likelihood Fields to Perform Sonar Scan Matching Localization," *Autonomous Robots*, vol. 26, no. 4, pp. 203–222, 2009.

[8] E. Pedrosa, A. Pereira, and N. Lau, "A Scan Matching Approach to SLAM with a Dynamic Likelihood Field," in *2016 International Conference on Autonomous Robot Systems and Competitions (ICARSC)*, May 2016, pp. 35–40.

[9] G. Grisetti, C. Stachniss, and W. Burgard, "Improved Techniques for Grid Mapping With Rao-Blackwellized Particle Filters," *Robotics, IEEE Transactions on*, vol. 23, no. 1, pp. 34–46, 2007.

[10] S. Thrun, "A Probabilistic On-Line Mapping Algorithm for Teams of Mobile Robots," *The International Journal of Robotics Research*, vol. 20, no. 5, pp. 335–363, 2001.

[11] S. Kohlbrecher, O. von Stryk, J. Meyer, and U. Klingauf, "A Flexible and Scalable SLAM System with Full 3D Motion Estimation," in *Proc. of the IEEE Int. Symp on Safety, Securitym and Rescue Robotics (SSRR)*, Kyoto, Japan, Nov. 2011, pp. 155–160.

[12] K. Madsen, H. Bruun, and O. Tingleff, "Methods for Non-Linear Least Squares Problems," Informatics and Mathematical Modelling, Technical University of Denmark, Tech. Rep., 2004.

[13] B. Triggs, P. F. McLauchlan, R. I. Hartley, and A. W. Fitzgibbon, "Bundle Adjustment — A Modern Synthesis," in *Vision Algorithms: Theory and Practice*, ser. Lecture Notes in Computer Science, B. Triggs, A. Zisserman, and R. Szeliski, Eds. Springer Berlin Heidelberg, 2000, vol. 1883, pp. 298–372.

[14] D. Fox, "Adapting the Sample Size in Particle Filters Through KLD-Sampling," *The International Journal of Robotics Research*, vol. 22, no. 12, pp. 985–1003, Dec. 2003.

[15] F. Lu and E. Milios, "Robot Pose Estimation in Unknown Environments by Matching 2D Range Scans," *Journal of Intelligent and Robotic Systems*, vol. 18, no. 3, pp. 249–275, 1997.

[16] A. Censi, "An ICP variant using a point-to-line metric," *2008 IEEE International Conference on Robotics and Automation (ICRA)*, pp. 19–25, 2008.

[17] A. Diosi and L. Kleeman, "Fast Laser Scan Matching using Polar Coordinates," *Int. J. Rob. Res.*, vol. 26, pp. 1125–1153, Oct. 2007.

[18] P. Biber and W. Strasser, "The normal distributions transform: a new approach to laser scan matching," in *Intelligent Robots and Systems, 2003. (IROS 2003). Proceedings. 2003 IEEE/RSJ International Conference on*, vol. 3. IEEE, 2003, pp. 2743–2748.

[19] M. Lauer, S. Lange, and M. Riedmiller, "Calculating the Perfect Match: an Efficient and Accurate Approach for Robot Self-Localization," in *Robocup 2005: Robot soccer world cup IX*. Springer, 2006, pp. 142–153.

[20] L. Dantanarayana, G. Dissanayake, and R. Ranasinge, "C-LOG: A Chamfer distance based algorithm for localisation in occupancy grid-maps ," *CAAI Transactions on Intelligence Technology*, vol. 1, no. 3, pp. 272–284, 2016.

[21] A. Censi, L. Iocchi, and G. Grisetti, "Scan matching in the hough domain," in *Robotics and Automation, 2005. ICRA 2005. Proceedings of the 2005 IEEE International Conference on*, 2005, pp. 2739–2744.

[22] K. Konolige and K. Chou, "Markov localization using correlation," in *Proceedings of the 16th international joint conference on Artificial intelligence - Volume 2*, ser. IJCAI'99. San Francisco, CA, USA: Morgan Kaufmann Publishers Inc., 1999, pp. 1154–1159.

[23] E. Olson, "Real-time correlative scan matching," in *Robotics and Automation (ICRA), 2011 IEEE International Conference on*, 2009, pp. 4387–4393.